



*Journal
of Ecological
Engineering*

ISSN 2299-8993



All issues

Volume 25, Issue 2, 2024



Impact of Salinity Stress and Zinc Oxide Nanoparticles on Macro and Micronutrient Assimilation: Unraveling the Link between Environmental Factors and Nutrient Uptake

Abhishek Singh, Rakesh Singh Sengar, Vishnu D. Rajput, Abdul Latief Al-Ghzawi, Uday Pratap Shahi, Karen Ghazaryan, Tatiana Minkina, Abdel Rahman Mohammad Al Tawaha, Omar Mahmoud Al Zoubi, Talaat Habeeb

J. Ecol. Eng. 2024; 25(2):1-9

DOI: <https://doi.org/10.12911/22998993/172947>

Abstract

Article (PDF)

Stats

Modeling of Dispersed Red 17 Dye Removal from Aqueous Solution Using Artificial Neural Network

Abdullah I. Ibrahim, Nabel K. Asmel, Waleed M. Sh. Alabdraba, Raid R. O. Al-Nima

J. Ecol. Eng. 2024; 25(2):10-19

DOI: <https://doi.org/10.12911/22998993/175673>

Abstract

Article (PDF)

Stats

Production and Use of Biogas and Biomethane from Waste for Climate Neutrality and Development of Green Economy

Yaroslav Gontaruk, Tetiana Kolomiets, Inna Honcharuk, Dina Tokarchuk

J. Ecol. Eng. 2024; 25(2):20-32

DOI: <https://doi.org/10.12911/22998993/175876>

Abstract

Article (PDF)

Stats

Enhancement of Medicago Sativa Plant Growth and Yield after Treatment with *Rhizobium* spp.

Muhammad I Massadeh, Emethal A. Alkhataibeh, Abdul Latif A. Al-Ghzawi, Fakher Aukour

J. Ecol. Eng. 2024; 25(2):33-43

DOI: <https://doi.org/10.12911/22998993/175874>

Abstract

Article (PDF)

Stats

Biosorption of Lead and Copper by Epiphytic Rhizobacterial Species Isolated from *Lepironia articulata* and *Scirpus grossus*

Fayeq Abdelhafez Al-Ajalín, Mushrifah Idris, Siti Rozaimah Sheikh Abdullah, Setyo Budi Kurniawan, Muhammad Fauzul Imron

J. Ecol. Eng. 2024; 25(2):44-61

DOI: <https://doi.org/10.12911/22998993/176144>

Abstract

Article (PDF)

Stats

Searching of Phenol-Degrading Bacteria in Raw Wastewater from Underground Coal Gasification Process as Suitable Candidates in Bioaugmentation Approach

Lukasz Jalowiecki, Jacek Borgulat, Aleksandra Strugała-Wilczek, Mikołaj Glaser, Grażyna Plaza

J. Ecol. Eng. 2024; 25(2):62-71

DOI: <https://doi.org/10.12911/22998993/176143>

Abstract

Article (PDF)

Stats

Decolorization of Cationic Dye from Aqueous Solution by Multiwalled Carbon Nanotubes

Salwa Hadi Ahmed, Ekehwanh A. Rasheed, Luma A. Rasheed, Firas R. Abdulrahim

J. Ecol. Eng. 2024; 25(2):72-84

DOI: <https://doi.org/10.12911/22998993/176210>

Abstract

Article (PDF)

Stats

The Emerging of Antibiotic Resistance Genes *sul1*, *tetA*, *bla_{GES}*, and *mexF* in Sapon Irrigation Canal and Aquaculture Pond in Kulon Progo Regency, Indonesia

Mohamad Aji Ikhrami, Dini Wahyu Kartika Sari, Masagus Muhammad Prima Putra

J. Ecol. Eng. 2024; 25(2):85-92

DOI: <https://doi.org/10.12911/22998993/176207>

Abstract

Article (PDF)

Stats

Estimating Greenhouse Gas Emissions from a Seafood Processing Facility

Nhi Thi Yen Nguyen, Giao Thanh Nguyen

J. Ecol. Eng. 2024; 25(2):93-102

DOI: <https://doi.org/10.12911/22998993/176250>

Abstract

Article (PDF)

Stats

Soil Textures-Based Evaluation of Horton and Philip's Infiltration Models for Equatorial Small Watersheds

Hendrik Pristianto, Suhardjono Suhardjono, Mohammad Bisri, Ery Suhartanto

J. Ecol. Eng. 2024; 25(2):103-114

DOI: <https://doi.org/10.12911/22998993/176319>

Abstract

Article (PDF)

Stats

Morpho-Physiological and Biochemical Responses of *Cymbopogon citratus* (DC.) and *Asparagus officinalis* L. to Waterlogging and Salinity Stress

Asma Hanif, Maida Sattar, Qin Qiushi, Mah Gul, Sobia Shahzad, Wei Jian, Muhammad Umair Hassan, Jameel Mohammed Al-Khayri, Mohammed Ibrahim Aldaej, Muhammad Naeem Sattar

J. Ecol. Eng. 2024; 25(2):115-125

DOI: <https://doi.org/10.12911/22998993/176474>

Abstract

Article (PDF)

Stats

Submit your paper

Instructions for Authors

All issues

Articles in press

Most read

Month Year

A Review of Microplastic Pollution: Harmful Effect on Environment and Animals, Remediation Strategies

Energy Inputs on the Production of Plastic Products

Heavy Metals – Definition, Natural and Anthropogenic Sources of Releasing into Ecosystems, Toxicity, and Removal Methods – An Overview Study

Indexes

Keywords index

Authors index

WYBRANE PRACE

Muhammad Rizky Romadhon, Mujiyo Mujiyo, Ongko Cahyono, Widyatmani Sih Dewi, Tiara Hardian, Akas Anggita, Khalyfah Hasanah, Viviana Irmawati, Nanda Mei Istiqomah

J. Ecol. Eng. 2024; 25(2):126-139

DOI: <https://doi.org/10.12911/22998993/176772>

[Abstract](#)

[Article \(PDF\)](#)

[Stats](#)

A Review of Microplastic Pollution: Harmful Effect on Environment and Animals, Remediation Strategies

Hamza Jasim Albazoni, Mohammed Jawad Salih Al-Haidarey, Afyaa Sabah Nasir

J. Ecol. Eng. 2024; 25(2):140-157

DOI: <https://doi.org/10.12911/22998993/176802>

[Abstract](#)

[Article \(PDF\)](#)

[Stats](#)

Diversity of Peritricha (Ciliophora) in Activated Sludge Depending on the Technology of Wastewater Treatment

Roman Babko, Tatiana Kuzmina, Volodimir Pilashechnik, Jacek Zaboruko, Joanna Szulżyk-Cieplak, Grzegorz Łagód

J. Ecol. Eng. 2024; 25(2):158-166

DOI: <https://doi.org/10.12911/22998993/175875>

[Abstract](#)

[Article \(PDF\)](#)

[Stats](#)

The impact of Air Pollution on the Number of Diagnosed Respiratory and Cardiovascular Diseases

Monika Wierzbńska, Aleksandra Kita

J. Ecol. Eng. 2024; 25(2):167-175

DOI: <https://doi.org/10.12911/22998993/176249>

[Abstract](#)

[Article \(PDF\)](#)

[Stats](#)

Analysis of Noise in Education Buildings

Józefa Wiater, Katarzyna Gładyszewska-Fiedoruk

J. Ecol. Eng. 2024; 25(2):176-181

DOI: <https://doi.org/10.12911/22998993/176142>

[Abstract](#)

[Article \(PDF\)](#)

[Stats](#)

Influence of Physico-Water and Retention Ability of Chosen Post-Industrial Waste Regarding Natural Use

Edyta Kruk, Sławomir Klatka, Marek Ryczek

J. Ecol. Eng. 2024; 25(2):182-189

DOI: <https://doi.org/10.12911/22998993/176145>

[Abstract](#)

[Article \(PDF\)](#)

[Stats](#)

Effect of Biostimulants on the Content and Uptake of Selected Macronutrients in Jerusalem Artichoke Tubers (*Helianthus tuberosus* L.)

Iwona Teresa Mystkowska, Aleksandra Dmitrowicz

J. Ecol. Eng. 2024; 25(2):190-202

DOI: <https://doi.org/10.12911/22998993/176248>

[Abstract](#)

[Article \(PDF\)](#)

[Stats](#)

Pogórze Przemyskie Landscape Park Complex as a Habitat for Rare and New to Poland Pinnularia Species

Teresa Noga, Jolanta Skubisz, Anita Poradowska

J. Ecol. Eng. 2024; 25(2):203-214

DOI: <https://doi.org/10.12911/22998993/176320>

[Abstract](#)

[Article \(PDF\)](#)

[Stats](#)

Efficacy of Compost and Vermicompost on Growth, Yield and Nutrients Content of Common Beans Crop (*Phaseolus vulgaris* L.)

Batool Al-Tawarah, Muawya A. Alasaf, Atif Y. Mahadeen

J. Ecol. Eng. 2024; 25(2):215-226

DOI: <https://doi.org/10.12911/22998993/176862>

[Abstract](#)

[Article \(PDF\)](#)

[Stats](#)

Ecological Approach to the Identification of the Degree of Phytophage Damage Based on Chlorophyll Fluorescence Induction in Oilseed Radish (*Raphanus sativus* L. var. *oleiformis* Pers.)

Yaroslav Tsytsiura

J. Ecol. Eng. 2024; 25(2):227-243

DOI: <https://doi.org/10.12911/22998993/176983>

[Abstract](#)

[Article \(PDF\)](#)

[Stats](#)

Optimization of Seaweed Harvesting for Maximum Antimicrobial Activity: Impact of Seasonal Variation, Temperature, and Salinity

Younes Farid, Loubna Jaatit, Mohammed Chennaoui

J. Ecol. Eng. 2024; 25(2):244-249

DOI: <https://doi.org/10.12911/22998993/176861>

[Abstract](#)

[Article \(PDF\)](#)

[Stats](#)

Effect of Auxin and Various Iron Concentrations on *Medicago × Varia* T. Martyn Yield and Forage Quality

Elżbieta Malinowska, Beata Wiśniewska-Kadzajan

J. Ecol. Eng. 2024; 25(2):250-256

DOI: <https://doi.org/10.12911/22998993/176946>

[Abstract](#)

[Article \(PDF\)](#)

[Stats](#)

Impact of Pharmaceuticals on the Individual Wastewater Treatment System

Małgorzata Helena Makowska, Marcin Spychała, Katarzyna Gajewska

J. Ecol. Eng. 2024; 25(2):257-266

DOI: <https://doi.org/10.12911/22998993/176945>

[Abstract](#)

[Article \(PDF\)](#)

[Stats](#)

WOOD FUELS

Bartosz Jan Ciupek, Rafal Urbaniak, Adam Nocoń

J. Ecol. Eng. 2024; 25(2):267-273

DOI: <https://doi.org/10.12911/22998993/177188>

[Abstract](#)

[Article \(PDF\)](#)

[Stats](#)

Ecotoxicological Hazard of Pesticide Use in Traditional Agricultural Technologies

Alla Lishchuk, Alla Parfenyk, Orest Furdychko, Vira Boroday, Iryna Beznosko, Oksana Drebot, Nadiya Karachinska

J. Ecol. Eng. 2024; 25(2):274-289

DOI: <https://doi.org/10.12911/22998993/177275>

[Abstract](#)

[Article \(PDF\)](#)

[Stats](#)

Briquettes from a Mixture of Cow Manure, Rice Husks and Wood Dust as Alternative Fuel

Teuku Athallah, Masykur Masykur, Hasanuddin Husin, Adib Adib, Muhammad Reza Aulia

J. Ecol. Eng. 2024; 25(2):290-299

DOI: <https://doi.org/10.12911/22998993/177194>

[Abstract](#)

[Article \(PDF\)](#)

[Stats](#)

Sugar Palm Starch/Chitosan Bionanocomposite Films Incorporated with Anthocyanin and Curcumin: Thermal Properties and Release Kinetics

Rachmina Rachmina, Muhammad Hasan, Uswatun Hasanah, Abdul Halim

J. Ecol. Eng. 2024; 25(2):300-308

DOI: <https://doi.org/10.12911/22998993/177140>

[Abstract](#)

[Article \(PDF\)](#)

[Stats](#)

Effect of Drying Temperature of Sawdust Biobriquettes with Used Lubricant Oil Adhesive Volume Variation over Carbonization Process

Rizka Wulandari Putri, Rahmatullah Rahmatullah, Budi Santoso, Aulia Savitri, Maulika Zahara

J. Ecol. Eng. 2024; 25(2):309-320

DOI: <https://doi.org/10.12911/22998993/174964>

[Abstract](#)

[Article \(PDF\)](#)

[Stats](#)

Biosorption of Hexavalent Chromium Cr(VI) onto Ziziphus Lotus Fruits Powder: Kinetics, Equilibrium, and Thermodynamics

Nosair El Yakoubi, Zineb Nejjar El Ansari, Mounia Ennami, Mohammed L'bachir El Kbiach, Loubna Bounab, Brahim El Bouzdoudi

J. Ecol. Eng. 2024; 25(2):321-332

DOI: <https://doi.org/10.12911/22998993/176571>

[Abstract](#)

[Article \(PDF\)](#)

[Stats](#)

Properties and Applications of Essential Oils: A Review

Zofia Durczyńska, Grażyna Żukowska

J. Ecol. Eng. 2024; 25(2):333-340

DOI: <https://doi.org/10.12911/22998993/177404>

[Abstract](#)

[Article \(PDF\)](#)

[Stats](#)

Reduction in Carbon Dioxide Production of Tropical Peatlands Under Nitrogen Fertilizer with Coal Fly Ash Application

Bambang Joko Priatmadi, Meldia Septiana, Ronny Mulyawan, Hairil Ifansyah, Abdul Haris, Afiah Hayati, Muhammad Mahbub, Akhmad R. Saidy

J. Ecol. Eng. 2024; 25(2):341-350

DOI: <https://doi.org/10.12911/22998993/177594>

[Abstract](#)

[Article \(PDF\)](#)

[Stats](#)



Ecological Approach to the Identification of the Degree of Phytophage Damage Based on Chlorophyll Fluorescence Induction in Oilseed Radish (*Raphanus sativus* L. var. *oleiformis* Pers.)

Yaroslav Tsytsiura^{1*}

¹ Vinnytsia National Agrarian University, Sonyachna St. 3, 21008 Vinnytsia, Ukraine

E-mail: yaroslavtsytsiura@ukr.net

ABSTRACT

The article presented describes a comprehensive study using chlorophyll fluorescence induction (CFI) as a non-destructive method for assessing phytophagous damage, particularly by cruciferous fleas, in oilseed radish (*Raphanus sativus* L. var. *oleiformis* Pers.) during early developmental stages. This method has been adapted for ecological monitoring and has implications for building ecological prognostic models. Several key parameters were measured and analyzed in relation to environmental stressors as well as plant damage, according to the basic indicators of the chlorophyll fluorescence induction curve (CFI) in relation to different gradations of cotyledon damage in the interval ‘traces of damage – 70% damage’ for three varieties. Typical CFI curves of cotyledons for different varieties of oilseed rape with different degrees of damage were constructed and its reliability (factor-dispersion and correlation schemes) was evaluated in the practice of indirect identification of adaptive plant response to the stress caused by pest damage with the assessment of the interaction of this damage with environmental parameters of the environment at different levels of stressfulness of the year from the standpoint of hydrothermal moisture regimes. This made it possible to expand the possibility of building ecological prognostic models for assessing the stress response systems of plant development in case of their damage in the early stages of growth processes. A decrease in the basic criteria of the chlorophyll fluorescence curve (F_0 , F_{pl} , F_m , F_{st}) in the range of 20.78–34.56% in the conjugate system damage degree-environmental stress of the period was established. This led to a decrease in the cotyledon water potential (Lwp) in the range of 3.7–41.2%, the plant viability index (RFd) in the range of 8.3–40.1%, and an increase in the indicator of endogenous (stress) factors (Kef) by 6.5–36.4%. On the basis of these studies, the possibility of using the chlorophyll fluorescence method for ecological and entomological analysis of the stress response of plants to the degree of damage to the primary assimilative cotyledonous tissues of plants at different levels of hydrothermal support during their growth period was proven.

Keywords: environmental stress response, crucifer flea beetles, damage degree, fluorescence method, photosystem activity.

INTRODUCTION

Oilseed radish (*Raphanus sativus* L. var. *oleiformis* Pers.) is a typical representative of the Brassicaceae family of multipurpose use (Tsytsiura, 2021). This species is particularly valuable for Ukraine, as it is considered from the point of view of bioenergy supply (Kaletnik and Lutkovska, 2020, Lutkovska and Kaletnik, 2020; Kaletnik et al., 2022; Tsytsiura, 2023, 2023a), green manure and biofumigation fertilization systems (Tsytsiura, 2023b) with a high

environmental stabilizing effect on intensive soil systems (Berezyuk et al, 2021; Tsytsiura, 2023c) as well as an active component of the biological defense system due to the allopathic effect and active glycoside compounds that can be used in the integrated defense system (Moskalets et al., 2023). The crops of the Brassicaceae family are quite attractive to many species of polyphagous and specific pests. There are about 90 different pest species that feed on the cruciferous crop group (Zheng et al., 2020). About 53 species of pests cause different kinds of damage to

oilseed radish crops. Of these, 29 species are specialized pests and the other 24 are polyphagous pests. These pests belong to 5 orders and 9 families. According to the results of multi-year assessments and studies of the entomocomplex of oilseed radish agrocenoses of different pre-sowing technological design (Tsytsiura, 2016, 2020), pests of such orders as beetles (*Coleoptera*), true bugs (*Hemiptera*), and lepidopterans (*Lepidoptera*) dominated among the represented families. For the sprouting – rosette period, the most harmful is the complex of crucifer flea beetles (*Phyllotreta*), which includes the following species: black flea beetles (*Phyllotreta atra* F.) (28–33.6% by number in the structure of flea species diversity), *Phyllotreta nemorum* L. (4.7–6.3%), *Phyllotreta undulata* Kutsch, (0.3–0.6%), *Phyllotreta nigripes* F. (53.4–61.5%), *Phyllotreta* F. (5.5–6.1%, respectively) (Tsytsiura, 2016; Gikonyo et al., 2019). It was determined that the decrease in yield of cruciferous crops from damage by various types of fleas at the seedling-rosette stage can reach an interval of 30–70%, depending on the degree of damage (Heath, 2017; Rasool & Lone, 2022). Given the fact that the primary and most important assimilation of cruciferous crops, including oilseed radish, is carried out by cotyledons, and the duration to the formation of the first pair of true leaves depending on climatic conditions can range from 6 to 20 days, the study of pest severity of crucifer flea beetles dominating the primary stage of plant growth processes is relevant (Heath, 2017). There is no doubt that the damage nature caused by crucifer flea beetles through destruction of cotyledon epidermis or deeper tissues with formation of characteristic ‘windows’ primarily affects the photosynthetic reactions and subsequent processes of the primary stages of dry matter accumulation during transition to formation of true leaves (Figure 1).

The damage to cotyledons by fleas causes disruption of the photosystem activity of its assimilation surface (Rasool & Lone, 2022). There was a definite link between the damage degree caused by the respective pest to the assimilating surface and the underlying physiological transformations in the plant organism’s photosystem (Pérez-Bueno et al., 2019; Arnold et al., 2023). Chlorophyll fluorescence is an indicator enabling to study the photochemical reactions in living objects related to the functioning of photosystem II (PS II), which is the most sensitive to environmental

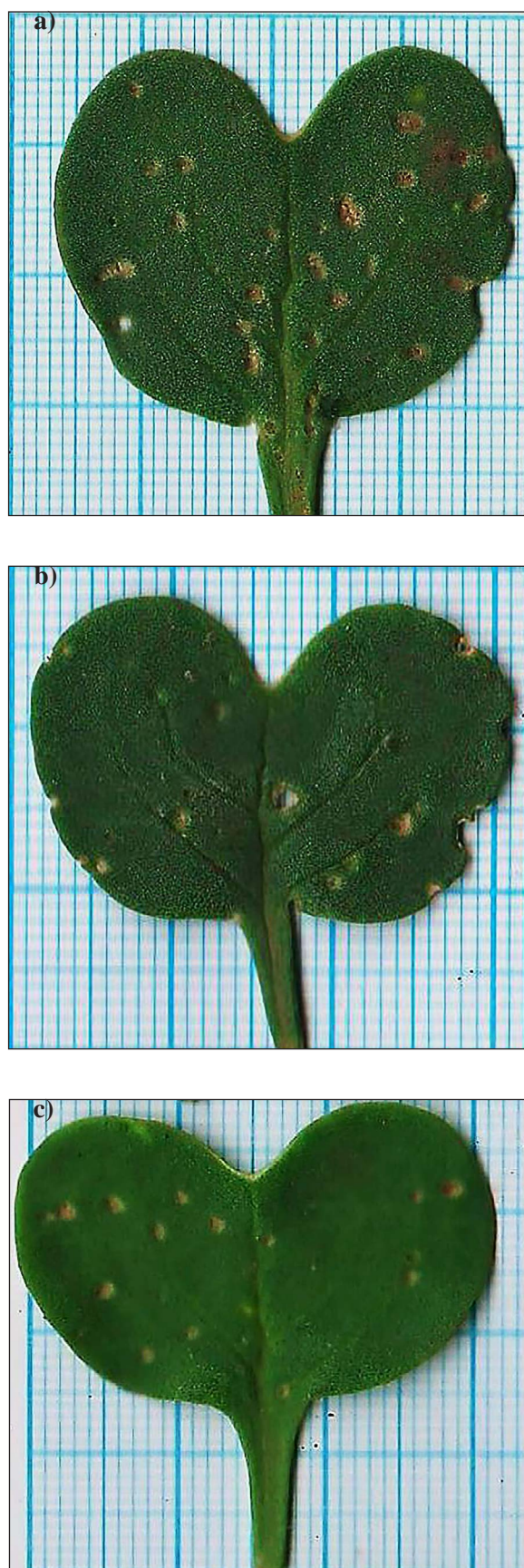


Figure 1. Damage nature of the oilseed radish cotyledon caused by crucifer flea beetles (a – ‘Raiduha’ variety, b – ‘Lybid’ variety, c – ‘Zhuravka’ variety)

factors. The findings on the curve of chlorophyll fluorescence intensity (CFI) contribute to a better understanding of the regulatory mechanisms that ensure efficient energy conversion in the primary and subsequent stages of photosynthesis (Kalaji et al. 2017; Sánchez-Moreiras et al. 2020). It was noted that the method of chlorophyll fluorescence in combination with the basic and derived indicators of the CFI reaction curve can be successfully used as a non-destructive method for assessing the overall stress resistance of plants to a wide range of factors, environmental adaptability and efficiency of agrochemicals of different nature in their cultivation technologies, as well as plant resistance to phyto- and entomophages (Moustakas et al., 2021). The importance of this method in terms of assessing pest damage in the early stages of plant vegetation is due to the possibility of its application to any type of plant. It requires a working portable fluorometer and predefined CFI curves on unaffected (undamaged) plants (Kalaji et al., 2016; Moustaka et al., 2023). This determines the low cost of this technique and its high adaptive and ecological orientation (Romanov et al., 2010; Amri et al., 2021). A certain disadvantage of this technique is the need for dark pre-adaptation of the assimilation apparatus of plants (Kalaji et al., 2017), which increases the duration of the determination itself. However, the methodology of this technique and its instrumental support are constantly being improved and, as a result, this duration is successfully reduced (Alonso et al., 2017). In comparison to the generally accepted methods of assessing damage to the assimilation apparatus, which involves eye examination or the use of damage scales (Parker et al., 2002), the accounting of chlorophyll fluorescence parameters allowed assessing not only the degree of damage but also analyzing the overall impact of such damage on the photosystem of plants of different species (Rolfe & Scholes, 2010; Pavlovic et al., 2014; Walters, 2015; Moustaka et al., 2023).

In confirmation of the above, the possibility of identifying the degree of phytophage pests' damage and harmfulness by assessing chlorophyll fluorescence induction was studied in a number of crops (de Souza et al., 2020; Moustaka et al., 2021; Holoborodko et al., 2022). Assessing the potential use of the chlorophyll fluorescence induction method to determine the pest damage of cruciferous crop sprouts on the example of oilseed radish plant had significant relevance as well as scientific novelty

and will improve the mechanisms for assessing interactions in pest-plant system based on basic physiological processes.

MATERIALS AND METHODS

The study was carried out during 2016–2023 on the experimental field of Vinnytsia National Agrarian University (N 49°11'31", E 28°22'16") on dark gray forest soils typical for the research area (type in the international qualification Luvic Greyic Phaeozem soils) with a weighted average humus content of 2.71%, mobile forms of nitrogen 79 mg kg⁻¹, phosphorus 184 mg kg⁻¹ and potassium 115 mg kg⁻¹ with the pH 5.7–6.0 of soil solution. In the first-middle of the second decade of April, three varieties of oilseed radish, 'Rayduga', 'Zhuravka', and 'Lybid' were sown with a recording plot area of 15 m² in 4-fold replications under a certain optimal variant of agrocenosis formation (Tsytsiura, 2020).

The hydrothermal conditions from sprouting to the rosette phase, corresponding to the period of active feeding and the highest level of harmfulness of crucifer flea beetles (Heath, 2017; Brockman, 2020) on oilseed radish crops as a typical representative of cruciferous crops were different (Table 1). Given a certain dependence of the harmfulness of cruciferous flea beetles on the hydrothermal conditions of the period of its active invasion of spring cruciferous crops (in the study area coincided late April – first decade of May increasing average daily temperatures on the background of a deficit of precipitation (Badenes-Pérez, 2018) years for the study period (based on the stress with regard to the risk of sprout damage intensity at the phenological stage of cotyledons), they were placed in the following order of growth 2021–2020–2019–2016–2022–2023–2017–2018 (Figure 2). The hydrothermal coefficient (HTC) was determined by Equation 1:

$$HTC = \frac{\sum R}{0.1 \times \sum t_{>10}} \quad (1)$$

where: $\sum R$ – the sum of precipitation (mm) over a period with temperatures above 10°C, $\sum t_{>10}$ – the sum of effective temperatures over the same period.

A 'Floratest' portable fluorometer was used to record the parameters of the chlorophyll fluorescence induction curve with a fixation duration

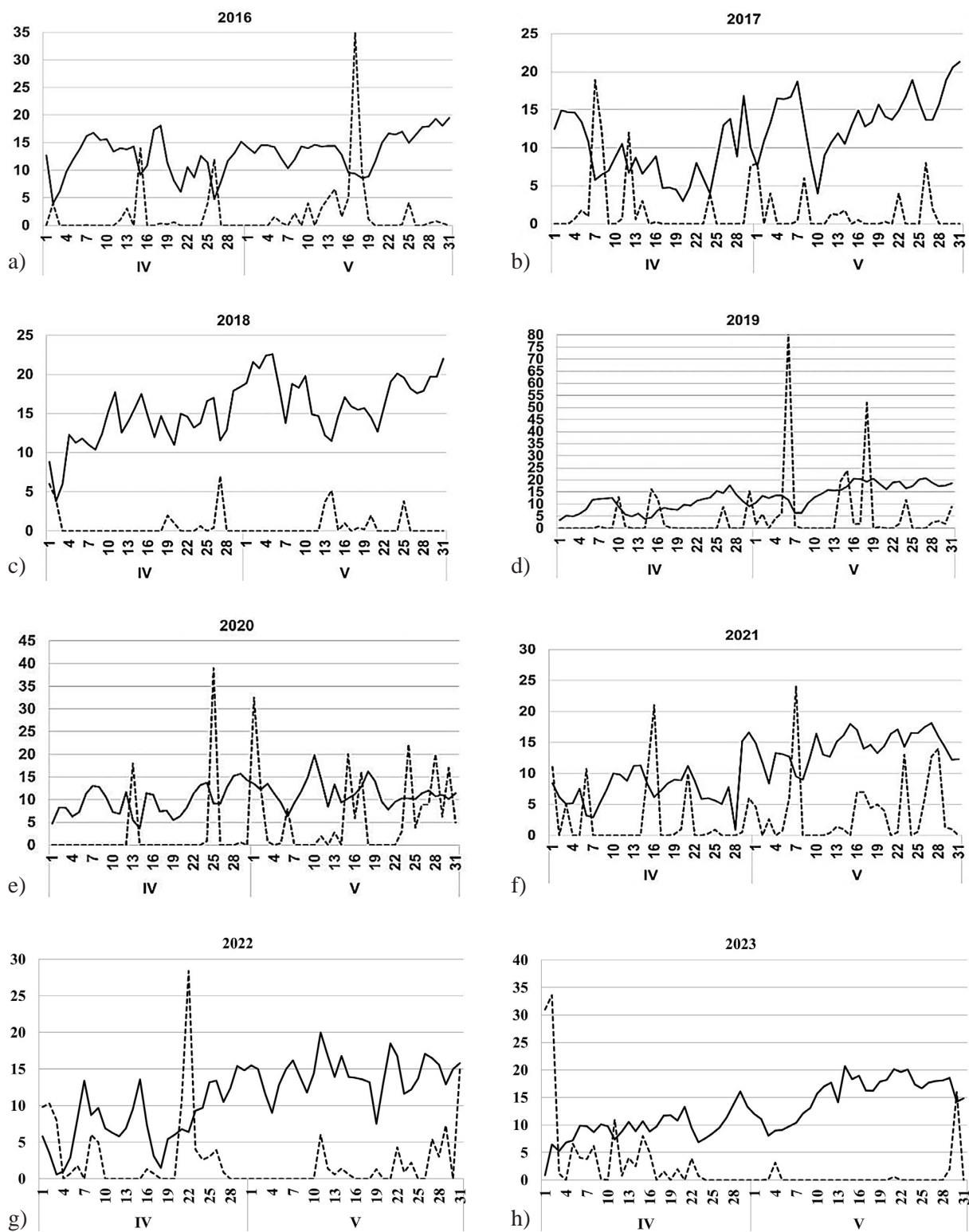


Figure 2. Dynamics of precipitation (mm – dotted line) and average daily temperature (°C – solid line) for the calendar germination period – formation of cotyledons and assimilation activity, 2016–2023

of 90 seconds after dark adaptation of cotyledons for 10 minutes in accordance with the basic technique for the device (Romanov et al., 2010; Tsytsiura, 2022). The device has a liquid crystal display (128×64 pixels) and an optoelectronic

sensor with an irradiation wavelength of 470 ± 15 nm, an irradiation area of a spot in the range of 4–15 mm² and an illumination within it of 2.4 W/m², a spectral range of fluorescence intensity measurements in the range from 670 to 800 nm,

Table 1. Hydrothermal conditions for the initial growth processes of oilseed radish during the full sprouting to rosette period, 2016–2021

Indicator	Years							
	2016	2017	2018	2019	2020	2021	2022	2023
The hydrothermal coefficient (HTC)	1.227	0.645	0.258	4.710	5.489	3.963	1.122	0.713

a functional measurement duration of 3 minutes and software for displaying data in tabular and graphical form. For the measurement, cotyledons were used at its full formation phase (BBCH 09–10) with the selection of 25 typical cotyledons at the level of damage of the assimilation

surface with 10%, 30%, 50% and 70% in each replication. The control variant had ‘traces of damage’. The damage degree was determined according to the visualized damage scale (Figure 3 a,b). The chlorophyll fluorescence parameters were counted at the combined damage by the

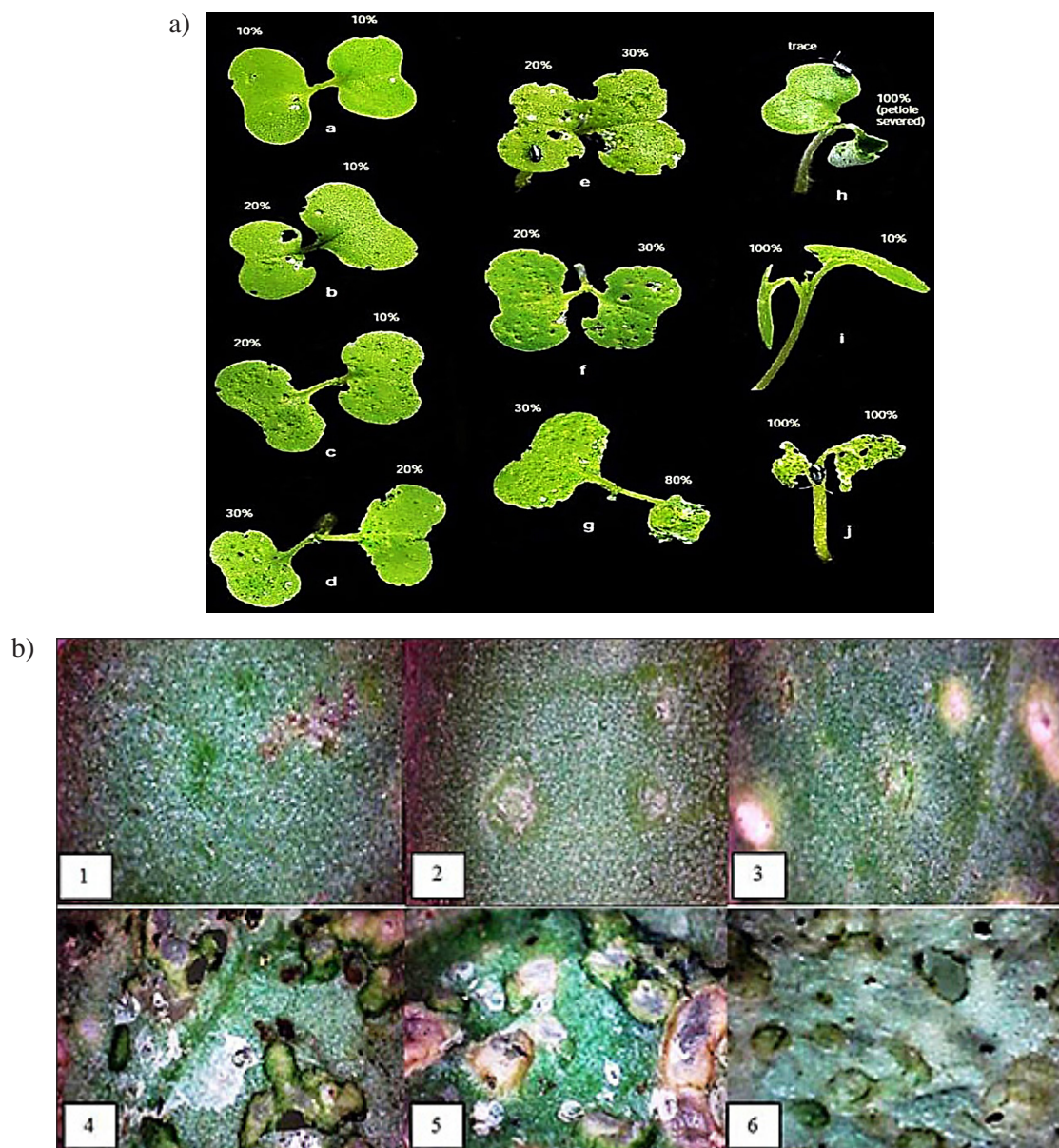


Figure 3. Visualized scale of (a) the damage degree of the assimilating surface of cotyledons (adapted by Soroka et al., 2011) and of (b) the damage degree of the assimilating surface of cotyledons (variety ‘Zhuravka’, photo sample for the period 2016–2023 (adapted by Soroka & Grenkow, 2013)). Percentage of damage: 1-traces of damage; 2–10%; 3–30%; 4–50%; 5–70%; 6–100% (complete discoloration)

following cruciferous flea beetle species: *Ph. atra* F., *Ph. nemorum* L., *Ph. undulata* Kutsch., *Ph. nigripes* F., *Ph. vitata* F. The measurements were based on the chlorophyll fluorescence induction curve (CFI) (Kautsky effect) (Figure 4). In the course of the experiments, the generally accepted indicators of the curve were analyzed (Brestic & Zivcak, 2013; Kalaji et al. 2017 (Table 2)): F_0 – minimal fluorescence, F_{pl} – value of fluorescence induction ‘plateau’, F_m – maximal fluorescence, F_{st} – fluorescence in steady state and complex of indicators (Table 3). The comparison of the variants (%) was calculated by using Equation 2:

$$k_{\text{comparison}} = \frac{k_1}{k_2} \times 100 \quad (2)$$

where: k_1 – indicator of the first variant, k_2 – indicator of the second variant.

For the statistical assessment of the obtained data, a system of ANOVA (LSD ($p < 0.05$)) analysis

was used, as well as variation (coefficient of variation (CV, %)) and correlation analysis according to generally accepted methods (Sneyd et al., 2022) with the use of the Statistica 10 statistical software (StatSoft – Dell Software Company, USA).

RESULTS AND DISCUSSION

The results of the research showed that the chlorophyll fluorescence induction rates had both a certain varietal specificity of formation and depended on the degree of cotyledons damage by the crucifer flea beetles. Thus, the intensity of the curve inclination on the F_{pl} – F_m area in the ‘Lybid’ was the highest among the studied varieties against the background of cotyledon dark adaptation with growth dynamics from 784 relative units of fluorescence between 10–11 seconds of fixation to 2100 relative units per 1 second of fixation,

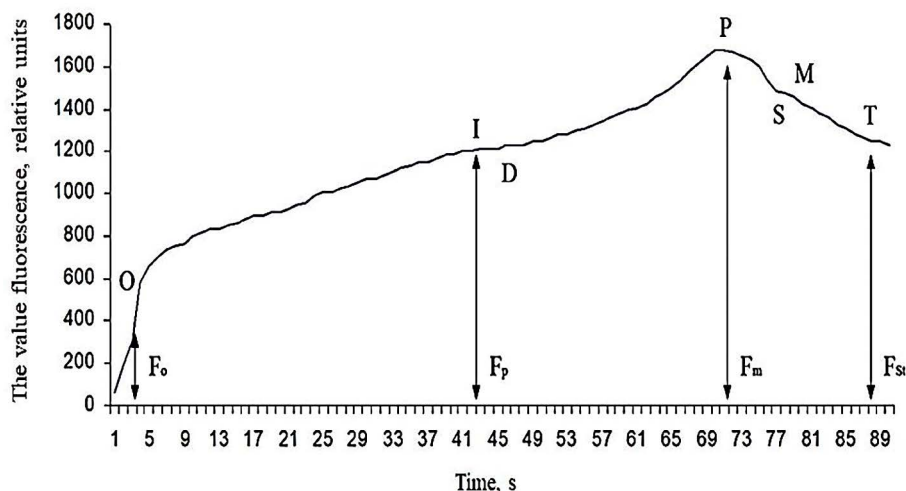


Figure 4. Typical chlorophyll fluorescence induction curve: F_0 is the initial value of fluorescence induction after irradiation is turned on; F_p (or F_{pl}) is the “plateau” fluorescence induction value; F_m is the maximum value of fluorescence induction; F_{st} is the stationary value of fluorescence induction after light adaptation of a plant leaf (Holoborodko et al., 2022)

Table 2. Characteristic segments of the chlorophyll fluorescence induction curve and their diagnostic significance (the data is grouped by Holoborodko et al. (2022))

The CFI segment	Type of the segment	Possible time interval, s	Stages of the photosynthetic process that this segment provides information about
Point O	initial segment	0–5	Efficiency of chlorophyll II light of reaction centers
O–I–D–P	exit to the main maximum	0.1–10.0 (0.1–1.0)	The electron transport link (from H_2O to PD (ferredoxin) and NADP) is the so-called ‘Light Stag’ of photosynthesis
P–S–M	descending and moving to the second maximum	3.0–50.0 (0.5–10.0)	Activation (via PD) of the Calvin cycle enzyme proteins, establishment of the pH gradient in membranes, reduction of competing acceptors (O_2 , NO etc.)
M–T	descending and entering stationary mode	10–2000 (10–300)	Adjustment of reactions in the Calvin cycle and flows of substances through membranes and through leaf vessels

Table 3. Derived index indicators of the CFI curve used in research (grouped on the basis of CFI curve application protocols in the analysis of plant stress response and pre-adaptation (Tsytisiura, 2022, 2023))

The CFI curve indexes	The applied Equation
Fluorescence rise	$dF_{pl} = F_{pl} - F_0$
Maximum variable fluorescence	$F_v = F_m - F_0$
Index of the effect of exogenous and endogenous factors	dF_{pl} / F_v
Photochemical efficiency or quantum efficiency (EP)	$EP = F_v / F_m$
Photochemical quenching (Q_{ue})	$Q_{ue} = F_0 / F_v$
Leaf water potential (L_{wp})	$L_{wp} = F_m / F_0$
Plant viability index (RF_d)	$RF_d = (F_m - F_{st}) / F_{st}$
Indicator of endogenous (stress) factors (K_{ef})	$K_{ef} = F_{st} / F_m$
Value of photochemical quenching of fluorescence (QP)	$QP = (F_m - F_{st}) / (F_m - F_0)$
Index of the efficiency of the primary reactions of photosynthesis (K_{pp})	$K_{pp} = F_v / F_0$
Fluorescence decay coefficient (K_{fd})	$K_{fd} = F_m / F_{st}$
Relative change of fluorescence at time t (V_t)	$V_t = (F_{st} - F_0) / (F_m - F_0)$

i.e. 65.8 relative units per 1 second of time fixation. A similar value was recorded for the ‘Raiduha’ variety at 63.8 with an interval shift of 11–12 and 27–28 seconds of fixation (Figure 5). The ‘Zhuravka’ variety had 48.0 with a similar

fixation time shift of 12–13 and 31–33 seconds, respectively. In spite of the time shift of growth amplitude fixation, the general reaching of the peak F_m value was observed at the interval of 20–21 seconds. The presence of a plateau-like area in

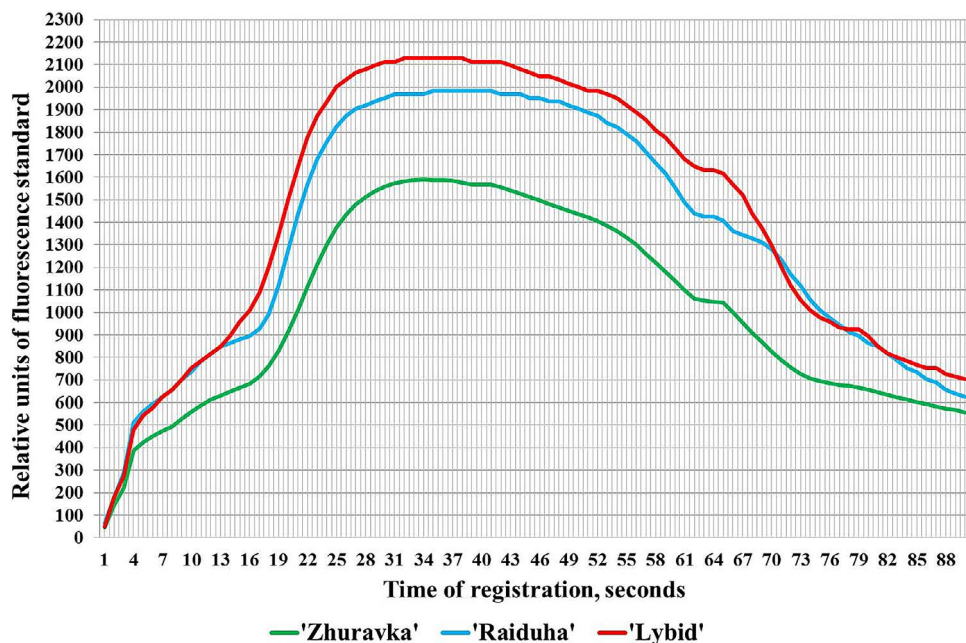


Figure 5. The nature of the CFI curve in oilseed radish varieties at the cotyledon phase (undamaged variant) based on the mean values at the time fixation points for the period 2016–2023

the interval of 62–65 seconds of fixation recorded for all varieties of oilseed radish. The level of minimum fluorescence (F_0) also had varietal characteristics with a minimum value in the ‘Zhuravka’ variety measuring 413 relative units, which is 26.2% lower than in the ‘Raiduha’ variety and 24.1% lower than in the ‘Lybid’ variety. The F_m value was significantly different, with a maximum value in the ‘Lybid’ variety and a minimum value in the ‘Zhuravka’ variety. The interval of the CFI curve at the F_0 – F_m was described as dynamically increasing with an intense decrease in the direction of the stationary fluorescence (F_{st}). It should be noted that the F_{pl} index was fixed on the dynamically changing part of the curve. According to Kalaji et al. (2017), this character indicates sensitivity to changes in census intensity due to a decrease in the concentration of chlorophyll in cotyledon tissues, which in turn increases the damage caused by fleas with an increase in plant density in the germination phase. It is known (de Souza et al., 2022) that the species with a higher amplitude of the CFI curve due to lower values of F_0 and F_{st} against the background of intensively growing F_m are more sensitive to the changes in the basic indicators of chlorophyll fluorescence induction to damage by pests and diseases of the leaf assimilation surface. Similar features have been noted in other studies under the influence of herbicides, which cause similar destruction of the photosynthetic surface of the leaf apparatus as flea damage (Kargar et al., 2019; de Souza et al., 2020). The possibility of such a prediction has been confirmed in a number of studies (Moustaka et al., 2021; Suárez et al., 2022; Arnold et al., 2023). On the basis of these generalizations, higher adaptive resistance in the flea-cotyledon photosystem system is expected in ‘Zhuravka’ than in ‘Lybid’. The changes in both basic and derived indices of chlorophyll fluorescence induction of cotyledons of oilseed radish varieties depending on the degree of their damage were also determined (Figure 6, Table 4) and it has confirmed the above-mentioned conclusions.

The data showed a consistent decrease in both the base indicators of the CFI curve and the calculated index derivatives for an increase in the degree of cotyledons damage. At the same time, the decrease in amplitude of the fast phase of chlorophyll fluorescence (F_0 – F_m section of the curve) and its slow phase (F_m – F_{st} section) with increasing degree of cotyledon damage differing in intensity among the varieties. The ‘Zhuravka’ variety showed a 1.61% increase in the fast phase of chlorophyll fluorescence and a

0.87% increase in its slow phase for 10% of cotyledon damage caused by crucifer flea beetles, compared to the control variant. Subsequently, an increase in damage degree led to a strong decrease in amplitude of both fast (by 19.11% – at 20% damage degree to 47.41% – at 70% damage degree) and slow phases of chlorophyll fluorescence (10.25% and 41.00%, respectively). For the ‘Lybid’ variety, a decrease in amplitude was noted already at 10% damage degree, 5.43% for fast and 4.21% for slow phases of chlorophyll fluorescence. At 70% damage level, the reduction was 62.88% and 60.04%, respectively. In comparison with the control variant, the overall reduction in the base values of the CFI curve for the 70% damage variant was, on average, 13.06% for F_0 , 37.66% for F_{pl} , 42.35% for F_m and 28.36% for F_{st} . The EP indicator showed a steady decline with 13.89–22.97% reduction to control in the marginal variants. The obtained results indicate the similarity of the cotyledon reaction, especially in the variant of damage in the range of 50-70% to the action of aggressive active ingredients of herbicides (Durigon et al., 2019). In other words, the system of combined feeding of flea beetles of the prickly-sucking and gnawing type (Heath, 2017) forms the effect of a necrotic tissue reaction, which increases along with damage. Minor damage in the form of punctures of the epidermis, small pit ulcers are characteristic of the damage level of 10-20%, which causes an intense change in color with an increase in the concentration of chlorophyll between the damage zones. This resulted in an increase in the basic indicators of IFH in the variant of 10% damage (Table 2, Figure 6). On the basis of study of Moustaka et al. (2021), these physiological processes in the cotyledons and the observed redistribution of chlorophyll at the level of up to 10% damage can be used for the above-mentioned identification of oil radish varieties resistant to cruciferous flea beetle. It has also been noted that intensive cotyledon parenchyma eating and the appearance of ‘windows’ causes the formation of continuous necrosis. As a result, this causes a violation of the basic physiological and assimilation processes in the cotyledons and leads to the process of induction of chlorophyll fluorescence according to the above-mentioned type of damage to the leaf apparatus by herbicides (Ali et al., 2022; Holoborodko et al. 2022), i.e., a certain identity of the action of phytophages and herbicides on the corresponding reaction

Table 4. Basic and estimated cotyledons CFI curve indicators in oilseed radish varieties (for the phenostage BBCH 10) depending on the damage degree caused by *Crucifer flea beetles* (relative fluorescence reference units), average for the 2016–2023 period

Damage degree, %	Basic indicators									Estimated indicators and indices							
	F_0	F_{pl}	F_m	F_{st}	dF_{pl}	F_v	dF_{pl}/F_v	EP	L_{wp}	Q_{ue}	RF_d	K_{st}	QP	K_{pp}	K_{fd}	V_t	
‘Zhuravka’ variety																	
Control	1*	413	630	1590	556	217	1177	0.18	0.74	3.85	0.35	1.86	0.35	0.88	2.85	2.86	0.121
	2	459	608	1503	511	149	1044	0.14	0.69	3.28	0.44	1.94	0.34	0.95	2.28	2.94	0.050
10	1	452	638	1648	605	186	1196	0.16	0.73	3.65	0.38	1.72	0.37	0.87	2.65	2.72	0.128
	2	471	612	1574	578	141	1103	0.13	0.70	3.34	0.43	1.72	0.37	0.90	2.34	2.72	0.097
30	1	440	590	1392	464	150	952	0.16	0.68	3.16	0.46	2.00	0.33	0.97	2.16	3.00	0.025
	2	451	563	1240	473	112	789	0.14	0.64	2.75	0.57	1.62	0.38	0.97	1.75	2.62	0.028
50	1	420	447	1200	438	27	780	0.03	0.65	2.86	0.54	1.74	0.37	0.98	1.86	2.74	0.023
	2	439	456	1078	447	17	639	0.02	0.59	2.46	0.68	1.41	0.42	0.99	1.46	2.41	0.013
70	1	405	416	1024	414	11	619	0.02	0.60	2.53	0.65	1.47	0.40	0.99	1.53	2.47	0.015
	2	421	432	896	426	11	475	0.02	0.53	2.13	0.88	1.10	0.47	0.98	1.13	2.10	0.011
‘Raiduha’ variety																	
Control	560	816	1984	624	256	1424	0.18	0.72	3.54	0.39	2.18	0.31	0.96	2.54	3.18	0.045	
10	592	864	2016	672	272	1424	0.19	0.71	3.41	0.42	2.00	0.33	0.94	2.41	3.00	0.056	
30	548	736	1776	598	188	1228	0.15	0.69	3.24	0.45	1.97	0.34	0.96	2.24	2.97	0.041	
50	464	548	1360	491	84	896	0.09	0.66	2.93	0.52	1.77	0.36	0.97	1.93	2.77	0.030	
70	446	496	1184	459	50	738	0.07	0.62	2.65	0.60	1.58	0.39	0.98	1.65	2.58	0.018	
‘Lybid’ variety																	
Control	544	784	2128	704	240	1584	0.15	0.74	3.91	0.34	2.02	0.33	0.90	2.91	3.02	0.101	
10	550	832	2048	684	282	1498	0.19	0.73	3.72	0.37	1.99	0.33	0.91	2.72	2.99	0.089	
30	532	704	1792	628	172	1260	0.14	0.70	3.37	0.42	1.85	0.35	0.92	2.37	2.85	0.076	
50	496	577	1424	549	81	928	0.09	0.65	2.87	0.53	1.59	0.39	0.94	1.87	2.59	0.057	
70	452	472	1040	471	20	588	0.03	0.57	2.30	0.77	1.21	0.45	0.97	1.30	2.21	0.032	
The share of influence of experimental factors																	
LSD_{05}		F_0	F_{pl}	F_m	F_{st}	factors				F_0	F_{pl}	F_m	F_{st}				
LSD_{05} factor A (year)		4.95	5.84	6.02	3.75	A				15.207	15.698	17.258	13.298				
LSD_{05} factor B (varieties)		2.85	3.37	3.47	2.17	B				16.369	18.325	20.411	20.789				
LSD_{05} factor C (degree of damage)		4.04	4.76	4.92	3.06	C				32.656	34.687	37.569	30.694				
LSD_{05} interaction AB		7.00	8.26	8.51	5.31	AB				3.259	2.897	4.561	5.694				
LSD_{05} interaction AC		9.90	11.68	12.03	7.51	AC				9.637	8.654	5.740	9.367				
LSD_{05} interaction BC		5.72	6.74	6.95	4.34	BC				9.908	8.741	7.963	8.267				
LSD_{05} interaction ABC		14.00	16.51	17.01	10.62	ABC				12.964	10.998	6.498	11.891				

Note: * Data 1 – for the period 2016–2021 period conditions. 2 – for 2018 period conditions, respectively.

centers of the photosystem of the tissues of the assimilation surface of plants was proven.

Such processes are also confirmed by the assessment of cotyledon tissue water content by the water potential index L_{wp} . In healthy and young leaves, this ratio is about 3–5 and its value can be about 1, depending on the degree of stress and response to it (Tsytisura, 2022, 2023). In the considered case, L_{wp} decreased from 9.41% for 10% damage to 33.53% for 70% damage on average for the varieties. These results confirmed

the study of Gikonyo et al. (2019), according to which damage by cruciferous fleas at the cotyledon stage increases the overall respiration rate, transpiration levels, as well as reduces the habitus and water content of tissues. Against the background of an intensive increase in average daily temperatures, the following processes cause crop death (Soroka & Grenkow, 2013). The adaptability of the species is also characterised by the relative fluorescence variable at time t V_t which showed the 71.97% decrease in the V_t level for the

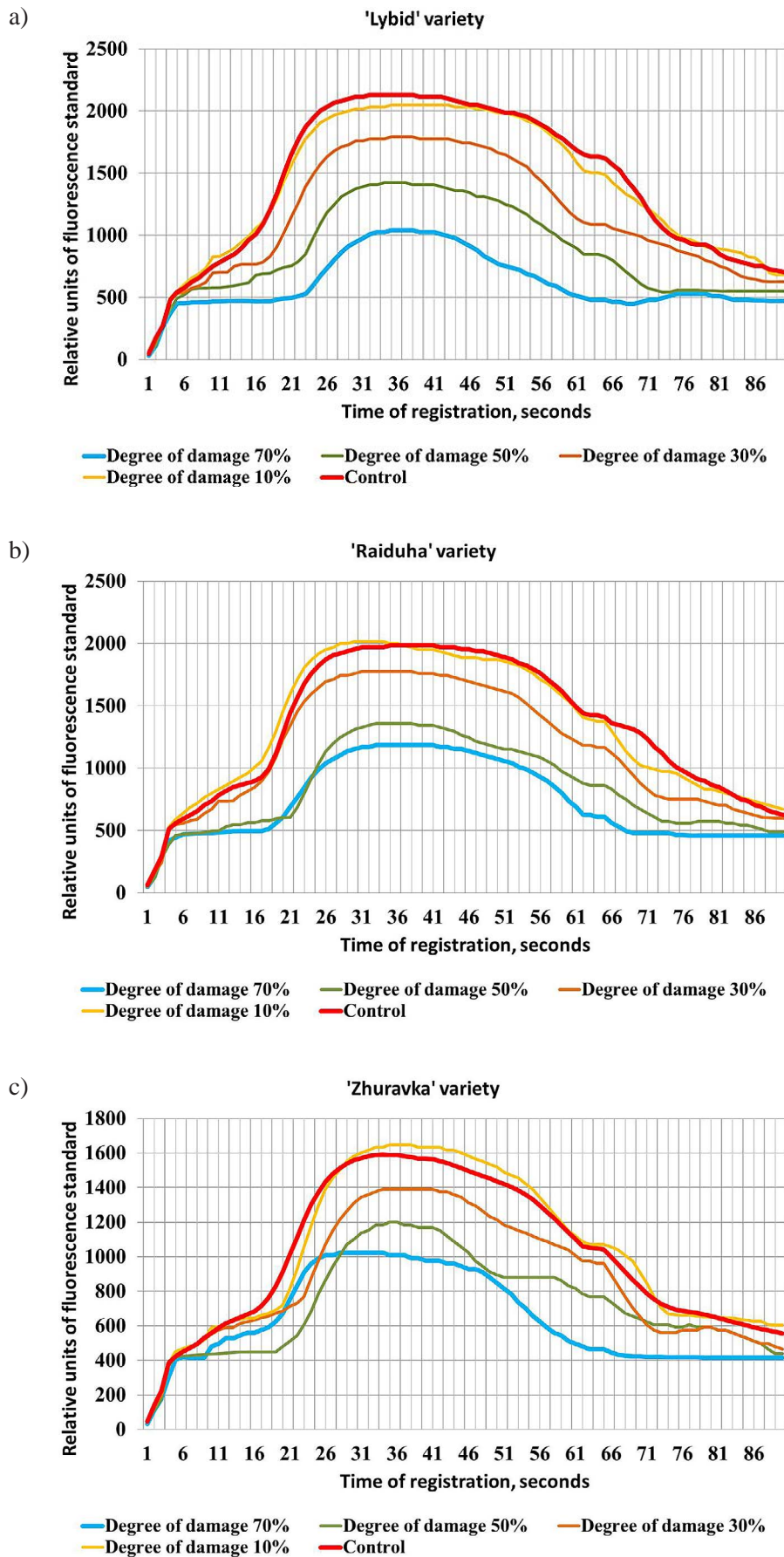


Figure 6. CFI curves of oilseed radish cotyledons depending on the damage degree caused by crucifer flea beetles according to combined data from 2016–2023

extreme cotyledon damage variants on average for varieties, indicating a significant decrease in the amplitude of the CFI curve over time of determination and with the detected reduced dynamics of the basic CFI curve indicators and increase in the overall stress state of the cotyledon photosystem. According to Brestic & Zivcak (2013) and Nies et al. (2021), this indicates an increase in the overall stress (reduction) state of the cotyledon photosystem. At the same time, an overall increase of 29.53% in the species viability index (RF_d) was observed. According to Kalaji et al. (2017), this indicator represents the threshold level of a stressful exogenous factor in interaction with environmental parameters. Given the different dynamics of reduction of RF_d within the control variant and the variant with the maximum damage of 70.0% varieties of resistance to damage caused by cruciferous flea beetles can be placed in the following order of decline ‘Lybid’ (reduction to the control 40.10%) – ‘Raiduha’ (38.00) – ‘Zhuravka’ (reduction 26.53%). The possibility of such gradation of varieties is confirmed by the results of the analysis of the influence of factors in the general system of variance analysis, where the ‘variety’ factor accounts for 16.37% for the F_0 indicator to 20.79% for the F_{st} indicator.

An increased stress-response of the oilseed radish plants for an increased degree of cotyledon damage and growth was determined, as compared to the control of such indicators as fluorescence decay coefficient (K_{fd}) (average growth for the varieties under study 25.49%), photochemical quenching level (Q_{uc}) (as an indicator of the influence of exogenous factors on the plant photosystem (Pérez-Bueno et al., 2019; Nies et al., 2021) (increase by 88.68%)) and photochemical fluorescence quenching index (QP) (increase by 7.45%). At the same time, the misbalance between the levels of growth of these values indicates negative changes in the primary reactions of photosynthesis, which is confirmed Kalaji et al. (2017) and a significant reduction of K_{pp} (by 45.56% on average for the studied varieties).

This dynamism of indicators was confirmed by a general decrease in the amplitude of cotyledon CFI curves with an increase in the percentage of damage (Figure 6). On the basis of the analysis, the following features were formulated with a consistent increase in the degree of flea damage a steady decrease in all basic indicators of the CFI curve; a gradual change in the path of the ‘plateau’ zone F_{pl} from the formation of the F_0 – F_m curve

section characteristic of the undamaged control to the formation of this section on a slowly growing or dynamically stagnating section of the CFI curve; a significant narrowing of the area from F_m to the beginning of the intensive decline of the CFI curve to the level of stationary fluorescence F_{st} ; a significant decrease in the value of the angular slope of the curve in the F_m – F_{st} area with the formation of a line with the fixation of similar induction values in the interval from 61 to 90 s of device operation. On the basis of the studies of Holoborodko et al. (2022), and Arnold et al. (2023), the identification response of the CFI curve to an increase in the degree of damage was confirmed. Under these conditions and taking into account the study of Ali et al. (2022), the threat of complete loss of functioning of the oilseed radish cotyledon photosystem was possible already at a damage level of 50%.

It has been noted (Heath, 2017; Brockman et al., 2020; Rasool & Lone, 2022) that drought conditions against the background of an intensive increase in average daily temperatures have a negative impact on the intensity of cotyledon assimilation tissue destruction. It was proven in the conducted studies that the intensity of the decrease in the main indicators of cotyledon chlorophyll fluorescence is based on the decrease in the hydrothermal coefficient during the period from germination to the formation of true leaves. The results of the analysis of variance of the data system, where year conditions represent 13.30 to 17.30% with this factor contributing to the interaction with others at 10.00 to 21.85% (Table 4), data for the variety ‘Zhuravka’ as the most resistant to flea damage for 2018 (as the most stressful with $HTC = 0.258$) were included. The results of this comparison allow concluding that the increased stress of the period of cotyledon formation of oilseed radish before the start of the true leaf apparatus functioning (from the period BBCH 11–13) increases the negative effect on the cotyledons photosystem at all the levels of damage under study. It is confirmed by peculiarities in the formation of the baseline indicators of the CFI curve for the 2018 conditions at $HTC 0.258$, compared to the annual average of assessments with the 2016–2023 average of $HTC 2.266$ (Table 1). There was an increase in F_0 from 2.50 to 11.14% depending on the degree of seedling damage. The value of F_{pl} was oscillatory between two periods, first decreasing between 3.49–4.58% in control and 30% damage, then

increasing between 2.01–3.85% with an increase in damage from 50 to 70%. Similar features were observed in the formation of F_{st} indicator. As for F_m indicator, its formation in the most stressful year showed the dynamics of stable decrease, in comparison with the long-term study cycle from 5.47% in the control to 12.50% in the variant with 70% of cotyledon damage. As a result, this nature of the formation of the basic indicators of the CFI curve inevitably influenced the calculated values of this curve by maintaining the same features as for the whole system of the multi-year study cycle, its overall reduction in the range 11.64–36.36%, depending on the specific indicator. Thus, a combinatorial property of the enhancing effect was noted on the cotyledons' photosystem of oilseed radish for the combination of low values of HTC during the period from seed germination to formation of true leaves and an increase in the degree of cotyledon damage caused by crucifer flea beetles. It reduced the amplitude of the CFI curve dynamics and the overall viability of plants at the seedling stage. Such results once again emphasize the similarity of the effect of flea damage to oilseed radish cotyledons with the effect of a number of active ingredients of herbicides, given the similarity of increasing the destructive effect of the plant photosystem along with aridization of climatic parameters (Durigon et al., 2019; de Souza et al., 2020; Ali et al., 2022).

The studies by Holoborodko et al. (2022) noted the presence of correlations between the CFI curve parameters and the degree of leaf damage by phytophages. Under these conditions, it was shown that an increase in the degree of cotyledons damage causes a change in the tightness of the relationship between the basic indicators of the CFI curve and even in the direction of the relationship (direct or inverse) between a number of estimated indicators (Table 5). Thus, the strength of the relationship between the initial fluorescence index (F_0) and its value in the 'plateau' zone F_{pl} (growth factor to control variant 1.89) and at steady-state level F_{st} (growth factor 1.67) increased significantly for 70% of seedling damage, reducing the relationship with the value of maximum fluorescence F_m (reduction factor 0.52). In contrast, the correlations between maximum fluorescence (F_m) and other baseline values decreased significantly (range of coefficient of decrease 0.66–0.97). Due to such correlations for an increase in the degree of cotyledons damage, there is a general decrease in the

significance of the relationships between the basic indicators of the CFI curve and the important derived (calculated) indicators, such as F_v , EP. This changes the direction of the relationship between leaf water potential (L_{wp}), plant viability index (RF_d) and increases the tightness of the fluorescence rate of change over time t (V_t).

The determined system of correlation dependencies between the basic indicators of the CFI curve of oilseed radish cotyledons, according to the generalizations of Kalaji et al. (2017), should be attributed to the consequential-parametric with a high degree of predicted variation. According to the results of Brestic & Zivcak (2013), the application of these correlation coefficients requires a systematic approach, taking into account the degree of cotyledon damage, the level of stress of abiotic environmental factors during pest feeding and the growth and development of oil radish plants. In comparison with similar estimates for other plant species (Holoborodko et al. 2022), where an inverse relationship between the degree of damage to the tissues of the assimilation surface of plants and the main indicators of the CFI curve was established, the nature of the relationship in the presented studies was heterogeneous, although with a dominant tendency to decrease the closeness of the relationship with increasing damage of cotyledons.

This is explained by the statements of Kalaji et al. (2017) from the standpoint of a complex mechanism of complementarity between the CFI curve indicators. This systematic dependence also explains the level of variation in the values of the CFI curve indicators in the context of accounting objects (Figure 7). It was based on the changes in variation in the CFI curve at each fixation point during the 90 second period of the fluorometer when the percentage of cotyledon damaged by cruciferous flea beetle was increasing (Figure 8). Thus, the variation of the CFI curve values by coefficient of variation (CV, %) on the control variant ranged from 17.6 to 41.3% with two extrema on the chart at 20 and 68 seconds. At the same time, the maximum increase in variation was observed in the F_0 - F_{pl} area and in a part of the F_m - F_{st} area, approaching precisely the level of the F_{st} value. An increase in cotyledon damage to the 70% level radically altered the nature of the variation in the cotyledon CFI curve estimates. With an overall decrease of the extrema variation to 36.1% and 30.7% at 38 and 79 seconds of fluorescence induction fixation by the device,

Table 5. Correlation analysis between baseline and index measures of the CFI curve as a function of the degree of cotyledons damage for the total data set of three varieties, 2016–2023 (for $N=300$)

Indicators		F_{pl}	F_m	F_{st}	dF_{pl}	F_v	dF_{pl}/F_v	EP	L_{ip}	Q_{le}	RF_d	K_d	QP	K_{pp}	K_d	V_i
F_0	1	0.480	0.775	0.566	0.074	0.651	-0.189	-0.428	-0.428	0.428	0.384	-0.385	0.531	-0.428	0.385	-0.531
	2	0.908	0.406	0.945	0.097	0.136	0.050	-0.341	-0.341	0.341	-0.285	0.285	-0.053	-0.341	-0.285	0.053
F_{pl}	1		0.653	0.818	0.863	0.658	0.629	0.078	0.078	-0.078	-0.046	0.046	-0.164	0.078	-0.046	0.164
	2		0.634	0.962	0.477	0.419	0.404	-0.017	-0.017	0.017	-0.028	0.027	-0.307	-0.017	-0.028	0.307
F_m	1			0.782	0.368	0.976	0.048	0.111	0.110	-0.111	0.430	-0.430	0.225	0.111	0.430	-0.225
	2			0.518	0.707	0.947	0.436	0.685	0.685	-0.685	0.691	-0.691	-0.284	0.685	0.691	0.284
F_{st}	1				0.633	0.786	0.359	0.103	0.103	-0.103	-0.095	0.094	-0.200	0.103	-0.094	0.200
	2				0.298	0.271	0.239	-0.161	-0.161	0.161	-0.202	0.202	-0.303	-0.161	-0.202	0.303
dF_{pl}	1					0.445	0.876	0.356	0.356	-0.356	-0.245	0.245	-0.499	0.356	-0.245	0.499
	2					0.760	0.926	0.674	0.674	-0.674	0.579	-0.579	-0.562	0.674	0.579	0.562
F_v	1						0.124	0.263	0.263	-0.263	0.402	-0.402	0.114	0.263	0.402	-0.114
	2						0.487	0.854	0.854	-0.854	0.841	-0.841	-0.300	0.854	0.841	0.300
dF_{pl}/F_v	1							0.306	0.306	-0.306	-0.395	0.395	-0.602	0.306	-0.395	0.602
	2							0.434	0.434	-0.434	0.317	-0.317	-0.611	0.434	0.317	0.611
EP	1								1.000	-1.000	0.067	-0.067	-0.500	1.000	0.067	0.500
	2								1.000	-1.000	0.929	-0.929	-0.277	1.000	0.929	0.277
L_{ip}	1									-1.000	0.067	-0.067	-0.500	1.000	0.067	0.500
	2									-1.000	0.929	-0.929	-0.278	1.000	0.929	0.278
Q_{le}	1										-0.067	0.067	0.500	-1.000	-0.067	-0.500
	2										-0.929	0.929	0.277	-1.000	-0.929	0.277
RF_d	1											-1.000	0.739	0.067	1.000	-0.739
	2											-1.000	-0.012	0.929	1.000	0.012
K_d	1												-0.739	-0.067	-1.000	0.739
	2												0.012	-0.929	-1.000	-0.012
QP	1													-0.500	0.739	-1.000
	2													-0.277	-0.012	-1.000
K_{pp}	1														0.067	0.500
	2														0.929	0.277
K_d	1															-0.739
	2															0.012

Note: Significant at 5%, 1%, 0.1% level probability, respectively for the value of correlation coefficients, apparently 0.113; 0.148; 0.188. *1, 2 – control variant and variant with stepwise reduction of 70% cotyledons damage, respectively.

respectively, the overall variation in the estimate of the complete CFI curve was higher by 7.7%. The maximum increase in variation was observed at the $F_0-F_{pl}-F_m$ areas of the CFI curve and the area closest to the steady-state fluorescence level F_{st} . The very nature of the variation coefficient curve at maximum cotyledons damage had a more pronounced oscillatory effect with a more complex pattern of variation and micro-oscillations within individual sections of the curve chart, which confirmed an increase in variation within the general population of data.

Destabilization of cotyledons photosystem activity due to crucifer flea beetle feeding

was confirmed, and also a rather significant sensitivity of cotyledon photosystem to environmental factors noted in the research Badenes-Pérez (2018) and Gikonyo et al. (2019) was indicated. The determined nature of the dynamics of variation of the CFI curve can also be explained by the study of Heath (2017), where it was noted that during cotyledon damage by cruciferous fleas in cotyledon tissues, there was an increase in respiration rate, peroxidase activity. As a result, the overall stress of the photosystem of the cotyledon assimilation surface increases, which is confirmed in the presented studies

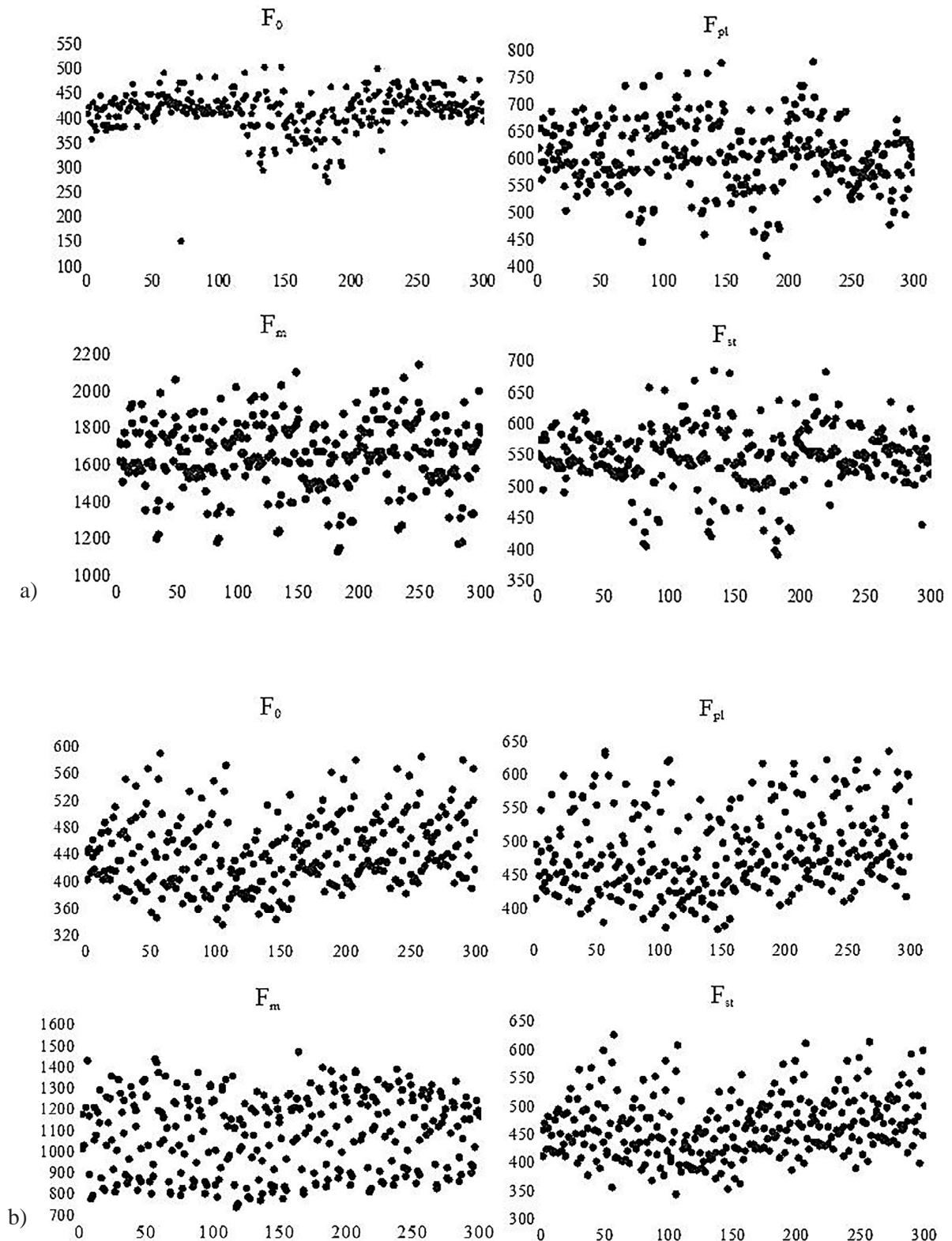


Figure 7. Dispersion chart of basic cotyledons CFI curve values for the combined total of observations (2016–2023, N = 300) for the three varieties (a–d – control variant; e–h variantis with 70% damage of cotyledons) (horizontal axis – sequence number in the combined group of observations, vertical axis – relative units of fluorescence)

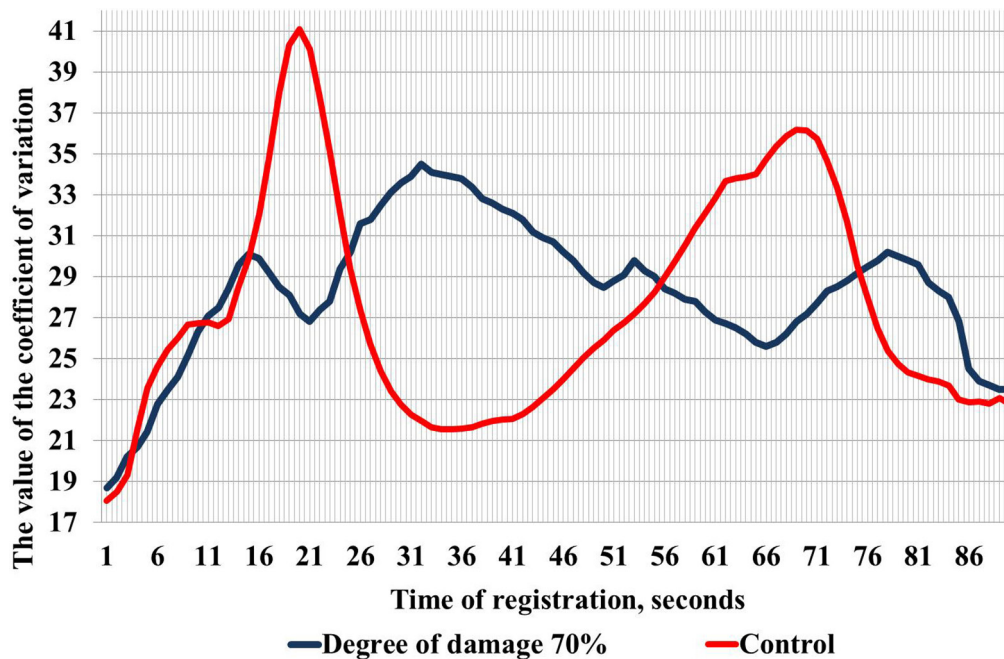


Figure 8. Value of the coefficient of variation (CV, %) of the CFI curve of oilseed radish cotyledons at each fixation point of the fluorometer depending on the degree of its damage caused by crucifer flea beetles (combined data for three varieties for the period 2016–2023)

by the overall increase in the average level of variation in physiologically important areas of the CFI curve.

CONCLUSIONS

The values of the main indicators of the chlorophyll fluorescence induction curve F_0 , F_{pl} , F_m , F_{st} and its calculated indices for cotyledons of different damage degree caused by crucifer flea beetles were statistically significant. This allows using this method to identify the degree of damage to cotyledons by seedling pests and to determine the resistant genotypes of oilseed radish (by analogy other cruciferous plant species) to different degrees of damage to the cotyledon apparatus. The above statements are based on the established correspondence of the percentage of cotyledon damage to the corresponding natural changes in the CFI curve, which, given the share of the factor ‘degree of damage’ in the overall discriminant system of the long-term research cycle at the level of 30.69–37.57% for the basic indicators of chlorophyll fluorescence induction and allow diagnosing the degree of cotyledon damage by pests without direct consideration, which is accepted in entomology.

REFERENCES

1. Ali L., Jo H., Choi S.M., Kim Y., Song J.T., Lee J.-D. 2022. Comparison of hyperspectral imagery and physiological characteristics of bentazone-tolerant and -susceptible soybean cultivars. *Agronomy*, 12, 2241. <https://doi.org/10.3390/agronomy12102241>
2. Alonso L., Van Wittenberghe S., Amorós-López J., Vila-Francés J., Gómez-Chova L., Moreno J. 2017. Diurnal cycle relationships between passive fluorescence, PRI and NPQ of vegetation in a controlled stress experiment. *Remote Sensing*, 9(8), 770. <https://doi.org/10.3390/rs9080770>
3. Amri M., Abbas Z., Trabelsi I., Ghanem M.E., Mentag R., Kharrat M. 2021. Chlorophyll content and fluorescence as physiological parameters for monitoring *Orobanche foetida* Poir. infection in faba bean. *PLoS ONE*, 16(5), e0241527. <https://doi.org/10.1371/journal.pone.0241527>.
4. Arnold A.L.M., McGrath C., Reinhardt A. 2023. Effects of oak processionary moth (*Thaumetopoea processionea* L.) outbreaks on the leaf performance and health of urban and forest oak trees (*Quercus robur* L.) in Brandenburg, Germany. *Forests*, 14(1), 124. <https://doi.org/10.3390/f14010124>
5. Badenes-Pérez F.R. 2018. Trap crops and insectary plants in the order brassicales. *Annals of the Entomological Society of America*, 112(4), 318–329, 2018. <https://doi.org/10.1093/aesa/say043>
6. Berezyuk S., Pryshliak N., Zubar I. 2021. Ecological

- and economic problems of fertilizers application in crop production. *Bulgarian Journal of Agricultural Science*, 27(1), 29–37.
7. Brestic M., Zivcak M. 2013. PSII fluorescence techniques for measurement of drought and high temperature stress signal in plants: protocols and applications. In: Rout G.R., Das A.B. (Eds.) *Molecular stress physiology of plants*. Springer Dordrecht, 87–131. https://doi.org/10.1007/978-81-322-0807-5_4
 8. Brockman R. 2020. Developing alternative practices for management of flea beetles attacking eggplant and leafy brassicaceous greens. Ph.D. Thesis. Kentucky Department of Agriculture Specialty Crop Block Grant. https://uknowledge.uky.edu/entomology_etds/59
 9. de Souza M.W.R., Ferreira E.A., dos Santos J.B., Soares M.A., de Castro e Castro B.M., Zanuncio J.C. 2020. Fluorescence of chlorophyll a in transgenic maize with herbicide application and attacked by *Spodoptera frugiperda* (Lepidoptera: Noctuidae). *Phytoparasitica*, 48(4), 567–573. <https://doi.org/10.1007/s12600-020-00816-5>
 10. Durigon M., Camera A., Cechin J., Vargas L., Chavarria G. 2019. Does spraying of atrazine on triazine-resistant canola hybrid impair photosynthetic processes? *Planta Daninha*, 37, 1–11. <https://doi.org/10.1590/S0100-83582019370100087>
 11. Gikonyo M.W., Biondi M., Beran F. 2019. Adaptation of flea beetles to Brassicaceae: host plant associations and geographic distribution of *Psylliodes latreille* and *Phyllotreta chevrolat* (Coleoptera, Chrysomelidae). *Zookeys*, 856, 51–73. <https://doi.org/10.3897/zookeys.856.33724>
 12. Heath J.R. 2017. Evaluation of flea beetle (*Phyllotreta* spp.) resistance in spring and winter-type Canola (*Brassica napus*). Ph.D. Thesis. University of Guelph, Ontario, Canada.
 13. Holoborodko K., Seliutina O., Alexeyeva A., Brygadyrenko, V., Ivanko I., Shulman M., Pakhomov O., Loza I., Sytnyk S., Lovynska V. 2022. The impact of *Cameraria ohridella* (Lepidoptera, Gracillariidae) on the state of aesculus hippocastanum photosynthetic apparatus in the urban environment. *International Journal of Plant Biology*, 13, 223–234. <https://doi.org/10.3390/ijpb13030019>
 14. Kargar M., Ghorbani R., Rashed Mohassel M.H., Rastgoo M. 2019. Chlorophyll fluorescence – a tool for quick identification of Accase and ALS inhibitor herbicides performance. *Planta Daninha*, 37, e019166813. <https://doi.org/10.1590/s0100-83582019370100132>
 15. Kalaji H.M., Jajoo A., Oukarroum A., Brestic M., Zivcak M., Samborska I.A., Cetner M.D., Łukasik I., Goltsev V., Ladle R.J. 2016. Chlorophyll a fluorescence as a tool to monitor physiological status of plants under abiotic stress conditions. *Acta Physiologiae Plantarum*, 38(102), 1–11. <https://doi.org/10.1007/s11738-016-2113-y>
 16. Kalaji H.M., Goltsev V.N., Žuk-Golaszewska K., Zivcak M., Brestic M. 2017. *Chlorophyll Fluorescence. Understanding Crop Performance: Basics and Applications*. CRC Press, Boca Raton.
 17. Kaletnik G., Lutkovska S. 2020. Strategic priorities of the system modernization environmental safety under sustainable development. *Journal of Environmental Management and Tourism*, 11, 5(45), 1124–1131. <https://doi.org/10.14207/ejsd.2021.v10n1p81>
 18. Kaletnik G., Pryshliak N., Khvesyk M., Khvesyk Ju. 2022. Legal regulations of biofuel production in Ukraine. *Polityka Energetyczna*. 25(1), 125–142. <https://doi.org/10.33223/epj/146411>
 19. Lutkovska S., Kaletnik G. 2020. Modern organizational and economic mechanism for environmental safety. *Journal of Environmental Management and Tourism*, 11, 3(43), 606–612. [https://doi.org/10.14505/jemt.11.3\(43\).14](https://doi.org/10.14505/jemt.11.3(43).14)
 20. Moskalets T., Pelekhata N., Svitelskyi M., Verheles P., Yakovenko R. 2023. Bacterial blight of viburnum (*Pseudomonas syringae* pv. *viburnum*): Biological features, causes, and consequences of manifestation, methods of control in the system of decorative and fruit gardening. *Scientific Horizons*. 26(5), 46–55. <https://doi.org/10.48077/scihor5.2023.46>
 21. Moustaka J., Meyling N.V., Hauser T.P. 2021. Induction of a compensatory photosynthetic response mechanism in tomato leaves upon short time feeding by the chewing insect *Spodoptera exigua*. *Insects*, 12(6), 562. <https://doi.org/10.3390/insects12060562>
 22. Moustaka J, Moustakas M. 2023. Early-Stage Detection of Biotic and Abiotic Stress on Plants by Chlorophyll Fluorescence Imaging Analysis. *Biosensors (Basel)*. 13(8), 796. doi: <https://doi.org/10.3390/bios13080796>
 23. Moustakas, M., Calatayud, A., Guidi, L. 2021. Chlorophyll fluorescence imaging analysis in biotic and abiotic stress. *Frontiers in Plant Science*, 12, 658500. <https://doi.org/10.3389/fpls.2021.658500>.
 24. Nies T., Niu Y., Ebenhöf O., Matsubara S., Matuszyńska A. 2021. Chlorophyll fluorescence: How the quality of information about PAM instrument parameters may affect our research. *bioRxiv*, e443801. <https://doi.org/10.1101/2021.05.12.443801>
 25. Parker B., Howard J., Binks R., Finch S., Jukes A. 2002. Brassicas: Biology and control of brassica flea beetles by integrating trap crops with insecticide use. HDC Final Rep. Project FV, 1–23.
 26. Pavlovic D., Nikolic B., Djurovic S., Anđelkovic A., Marisanvljevic D. 2014. Chlorophyll as a measure of plant health: Agroecological aspects. *Pestic Phytomedicine*, 29, 21–34. <https://doi.org/10.2298/PIF1401021P>.

27. Pérez-Bueno M.L., Pineda M., Barón M. 2019. Phenotyping plant responses to biotic stress by chlorophyll fluorescence imaging. *Front. Plant Sci*, 10, 1135. <https://doi.org/10.3389/fpls.2019.01135>
28. Rasool R., Lone G.M. 2022. Seasonal incidence of striped flea beetle *Phyllotreta striolata* F. on cruciferous crops in North Kashmir. *Indian Journal of Entomology*, e21120. <https://doi.org/10.55446/IJE.2021.137>
29. Rolfe S.A., Scholes J.D. 2010. Chlorophyll fluorescence imaging of plant-pathogen interactions. *Protoplasma*, 247, 163–175. <https://doi.org/10.1007/s00709-010-0203-z>
30. Romanov V.A., Galelyuka I.B., Sarakhan V. 2010. Portable fluorometer Floratest and specifics of its application. *Sensor Electronics and Microsystem Technology*, 7(3), 39–44. <https://doi.org/10.18524/1815-7459.2010.3.114470>
31. Sánchez-Moreiras A.M., Graña E., Reigosa M.J., Araniti F. 2020. Imaging of chlorophyll a fluorescence in natural compound-induced stress detection. *Frontiers in Plant Science*, 11, e583590. <https://doi.org/10.3389/fpls.2020.583590>
32. Sneyd J., Fewster R.M., McGillivray D. 2022. *Mathematics and Statistics for Science*; Springer Nature Switzerland AG: Cham, Switzerland. <https://doi.org/10.1007/978-3-031-05318-4>
33. Soroka J.J., Holowachuk J.M., Gruber M.Y., Grenkow L.F. 2011. Feeding by flea beetles (Coleoptera: Chrysomelidae; *Phyllotreta* spp.) is decreased on canola (*Brassica napus*) seedlings with increased trichome density. *Journal of Economic Entomology*, 104(1), 125–136. <https://doi.org/10.1603/EC10151>
34. Soroka J., Grenkow L. 2013. Susceptibility of Brassicaceous plants to feeding by flea beetles, *Phyllotreta* spp. (Coleoptera: Chrysomelidae). *Journal of Economic Entomology*, 106(6), 2557–2567. <https://doi.org/10.1603/ec13102>
35. Suárez J.C., Vanegas J.I., Contreras A.T., Anzola J.A., Urban M.O., Beebe S.E., Rao I.M. 2022. Chlorophyll fluorescence imaging as a tool for evaluating disease resistance of common bean lines in the Western Amazon Region of Colombia. *Plants (Basel)*, 11(10), e1371. <https://doi.org/10.3390/plants11101371>
36. Tsytsiura Y.H. 2016. Dynamics of pest infestation of oilseed radish crops in the Right-Bank Forest-Steppe of Ukraine. *Collection of scientific works of Uman National University of Horticulture. Part 1. Agricultural Sciences*, 89, :242–251. [in Ukrainian].
37. Tsytsiura Y.H. 2020. Modular-vitality and ideotypical approach in evaluating the efficiency of construction of oilseed radish agrophytocenosises (*Raphanus sativus* var. *oleifera* Pers.). *Agraarteacus*, 31(2), 219–243. <https://doi.org/10.15159/jas.20.27>
38. Tsytsiura Y.H. 2021. Selection of effective software for the analysis of the fractional composition of the chaotic seed layer using the example of oilseed radish. *Engenharia Agrícola, Jaboticabal*, 41(2), 161–170. <https://doi.org/10.1590/1809-4430-Eng.Agric.v41n2p161-170/2021>
39. Tsytsiura Y. 2022. Chlorophyll fluorescence induction method in assessing the efficiency of pre-sowing agro-technological construction of the oilseed radish (*Raphanus sativus* L. var. *oleiformis* Pers.) agrocecnosis. *Agronomy Research*, 20(3) 682–724. <https://doi.org/10.15159/ar.22.062>
40. Tsytsiura Y. 2023. Assessment of the relation between the adaptive potential of oilseed radish varieties (*Raphanus sativus* L. var. *oleiformis* Pers.) and chlorophyll fluorescence induction parameters. *Agronomy Research*, 20(1), 193–221. <https://doi.org/10.15159/AR.23.001>
41. Tsytsiura Y. 2023a. Evaluation of oilseed radish (*Raphanus sativus* l. var. *oleiformis* Pers.) oil as a potential component of biofuels. *Engenharia Agrícola, Jaboticabal*, 43(sp. iss.), e20220137. <http://dx.doi.org/10.1590/1809-4430-Eng.Agric.v43nepe20220137/2023>
42. Tsytsiura Y. 2023b. Estimation of biomethane yield from silage fermented biomass of oilseed radish (*Raphanus sativus* l. var. *oleiformis* Pers.) for different sowing and harvesting dates. *Agronomy Research*, 21(2), 940–978. <https://doi.org/10.15159/AR.23.101>
43. Tsytsiura Y. 2023c. Possibilities of using FijiImagej2, WipFrag and Basegrain programs for morphometric and granulometric soil analysis. *Engenharia Agrícola, Jaboticabal*, 43(6), e20230101. <http://dx.doi.org/10.1590/1809-4430-Eng.Agric.v43n6e20230101/2023>
44. Walters D.R. 2015. Photosynthesis in attacked plants and crops. In: *Physiological Responses of Plants to Attack. Crop & Soil Systems Research Group SRUC Edinburgh*, (Eds Walters D.R.), Wiley-Blackwell, UK.
45. Zheng X., Koopmann B., Ulber B., von Tiedemann A. 2020. A global survey on diseases and pests in oilseed rape-current challenges and innovative strategies of control. *Frontiers in Agronomy*, 2, e 590908. <https://doi.org/10.3389/fagro.2020.590908>